Marker-Free Coil-Misalignment Detection Approach Using TMR Sensor Array for Dynamic Wireless Charging of Electric Vehicles

Xuyang Liu[1], Wei Han[1], Chunhua Liu[2], and Philip W. T. Pong[1]

[1]Department of Electrical and Electronic Engineering, The University of Hong Kong, Hong Kong
[2]School of Energy and Environment, City University of Hong Kong, Hong Kong

This paper presents an approach to detect the lateral coil misalignment for the dynamic wireless charging system using a tunneling magnetoresistive (TMR) sensor array. The component of the magnetic field generated from the transmitting coil can directly provide the information of the coil misalignment between transmitting and receiving coils. A sensor array composed of 15 uniaxial TMR sensors was implemented to measure the vector magnetic field for detecting the coil misalignment. Both 3-D finite-element method modeling and experimental results over a relatively large misalignment range were presented to substantiate the effectiveness and feasibility of the proposed approach.

***Index Terms*— Coil misalignment, dynamic wireless charging (DWC), magnetic field measurement, tunneling magnetoresistive (TMR) sensor.**

I. Introduction

DYNAMIC wireless charging (DWC) technology for electric vehicles (EVs) has obtained an increasing attention recently [1], [2] because it enables on-road EVs to be powered wirelessly so that the EV driving range can be further extended. However, one main problem of the DWC system is that the receiving coils mounted on an EV should be well aligned with the transmitting coil embedded under lane in order to maximize the efficiency of energy transfer [3]. The output power and energy transmission efficiency drop significantly when there exists a large misalignment between the receiving and transmitting coils. Therefore, a cost-effective and reliable coil-misalignment detection approach is highly desired for the DWC system of EVs.

The existing vehicle-tracking techniques can be classified into two categories: marker-based approach and marker-free approach. The marker-based approach typically uses the radio-frequency identification (RFID) reader or magnetic sensor to detect the RFID tags or magnetic markers over/under lane [4]–[6]. However, the dense configuration of RFID or magnetic markers leads to high construction costs. The marker-free approach can overcome this drawback. Currently, the marker-free approach is implemented with search coils that are installed underneath a vehicle body to detect the lateral misalignment; however, search coils suffer from their complicated installation (due to an out-of-plane configuration) and bulky size (due to a large turn number) [7], [8]. The algorithm to determine the misalignment position by observing the change in voltage phase of search coil is unreliable and time consuming [7]. Furthermore, its actual applicability is largely restricted by the nonlinear relationship between the coil misalignment position and search-coil voltage.

Manuscript received March 16, 2018; revised May 28, 2018; accepted June 2, 2018. Date of publication June 26, 2018; date of current version October 17, 2018. Corresponding authors: C. Liu and P. W. T. Pong (e-mail: chualiu@eee.hku.hk; ppong@eee.hku.hk).

Color versions of one or more of the figures in this paper are available online at http://ieeexplore.ieee.org.

Digital Object Identifier 10.1109/TMAG.2018.2844863

In this paper, a marker-free approach to detect the lateral coil misalignment for the DWC system using a tunneling magnetoresistive (TMR) sensor array is proposed. TMR sensors are well qualified in the DWC operation due to their multiple features such as higher sensitivity, lower power consumption, excellent thermal stability, and large operating field range [9], [10]. The compact-in-size TMR sensor array in-plane with the receiving coil is employed to detect the magnetic field generated by the transmitting coil and then to determine the coil misalignment position, which makes the installation of sensor array convenient. Most importantly, the computation process is straightforward, and the lateral coil misalignment position can be directly obtained by analyzing the output amplitude of the TMR sensor array. Section II describes the fundamental principle of coil-misalignment detection. A 3-D finite-element method (FEM) simulation is performed to validate the principle in Section III. The experimental verification is provided in Section IV to further verify the feasibility of the proposed approach. Section V finally addresses a conclusion.

II. Working Principle of Coil-Misalignment Detection

The magnetic field distribution on the plane of receiving coil directly provides the coil-misalignment information. Fig. 1 shows the concept of the proposed coil-misalignment detection approach for a DWC system, which mainly focuses on the lateral misalignment detection. A magnetic sensor array is employed to measure the y-axis component of magnetic field on the plane of receiving coil and to determine the misalignment position.

Magnetic resonant coupling (MRC)-based wireless power transfer (WPT) technology has become more popular for implementing a DWC system for the moving EVs [11]–[13]. Fig. 2(a) shows the circuit schematic of the MRC-based WPT system adopting the series–series topology, which consists of the transmitter unit and the receiver unit, where R_t and R_r are the internal resistances of the transmitting and receiving coils, respectively, R_L is the load resistance, C_t and C_r

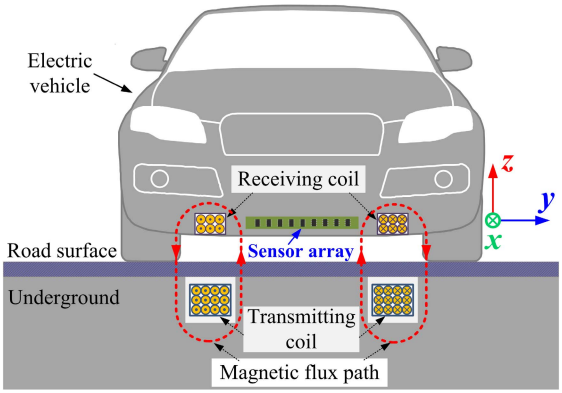

Fig. 1. Concept of coil-misalignment detection in a DWC system.

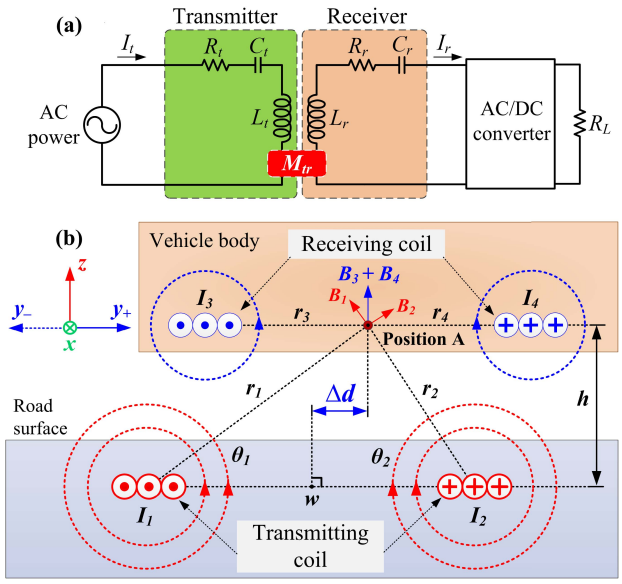

Fig. 2. (a) Circuit schematic of the MRC-based WPT system. (b) Diagram of magnetic field distribution at position A on the plane of receiving coil. There exists a lateral misalignment (Δd) between the receiving coil and the transmission coil.

are the compensated capacitors connected in series with the transmitting and receiving coils, respectively, and L_t and L_r are the self-inductance of the transmitting and receiving coils, respectively.

The transferred power and power transfer efficiency are highly dependent on the mutual inductance M_{tr} that is defined as the number of flux linking with the receiving coil due to the current through the transmitting coil. A larger M_{tr} facilitates more effective power transfer. M_{tr} can be determined by the double integral Neumann formula [14]

$$M_{\text{tr}} = k_{\text{tr}}\sqrt{L_t l_r} = \frac{\mu_0}{4\pi}\oint_t\oint_r \frac{dl_t dl_r \cos\varepsilon}{d_{\text{tr}}} \tag{1}$$

where k_{tr} is the coupling coefficient indicating the degree of coupling strength, dl_t and dl_r are the infinitesimal segments of the transmitting and receiving coils, respectively, and d_{tr} and ε are the distance and angle between two segments, respectively. Hence, a large lateral coil misalignment leads to the significant decrease of M_{tr}, thus lower power transfer efficiency.

Fig. 2(b) shows a diagram of magnetic field distribution at the sensing position A on the plane of receiving coil. The magnetic field generated from both transmitting and receiving coils at position A can be expressed as

$$\vec{B}_A = \vec{B}_1 + \vec{B}_2 + \vec{B}_3 + \vec{B}_4. \tag{2}$$

Hence, the y-axis direction component (B_y) of the magnetic field at position A can be expressed as

$$B_y = \vec{B}_y^1 + \vec{B}_y^2 + \vec{B}_y^3 + \vec{B}_y^4. \tag{3}$$

As position A is on the plane of receiving coil, the y-axis component of the magnetic field generated from the receiving coil is zero (i.e., $\vec{B}_y^3 = \vec{B}_y^4 = 0$), where B_y can be written as

$$B_y = \vec{B}_y^1 + \vec{B}_y^2. \tag{4}$$

Assuming the transmitting coil cable as a straight wire, and according to the Biot–Savart law, B_y at position A can be approximately calculated by [8]

$$\begin{aligned} B_y &= \frac{n\mu_0 I_1}{2\pi r_1}\sin\theta_1 - \frac{n\mu_0 I_2}{2\pi r_2}\sin\theta_2 \\ &= \frac{n\mu_0 I_t}{2\pi}\left(\frac{\sin\theta_1}{r_1} - \frac{\sin\theta_2}{r_2}\right) \end{aligned} \tag{5}$$

where n is the turn number of the transmitting coil, I_t is the current through the transmitting coil ($I_1 = I_2 = I_t$), r_1 and r_2 are the distances between position A and the transmitting coils, and θ_1 and θ_2 are the angles between the plane of transmitting coil and the line connecting sensing position A with transmitting coils.

From (5), the magnetic field distribution (B_y) highly depends on the lateral position of receiving coils. There exists a sensing position on the plane of receiving coil where the magnitude of B_y is zero. The lateral misalignment [Δd in Fig. 2(b)] of the receiving coil will lead to the lateral shift of B_y distribution on the plane of receiving coil, and thus the zero-field position. Therefore, it is possible to determine the coil misalignment (Δd) by detecting the position where B_y is zero.

By adopting the typical DWC parameters [15], the width (w) of transmitting coil is set to 0.8 m, the horizontal offset between the transmitting and receiving coils as 0.2 m, and the current flowing through the transmitting coil as 100 A_{rms}. The calculated magnitudes of B_y according to (5) is in the order of hundreds of microtesla. The DWC system uses 10–100 kHz operating frequency. Hence, it is feasible to employ a TMR magnetic sensor array to measure the magnetic field distribution due to its advantages of high sensitivity, good linearity, compact size, and wide bandwidth. Therefore, the lateral misalignment can be determined by locating the point on a TMR sensor array where minimal (near zero) magnetic field is measured.

III. Simulation Validation

A 3-D FEM simulation of the magnetic field distribution on the plane of receiving coil was performed to validate the magnetic field calculation model. Fig. 3(a) and (b) shows the dimensions of the transmitting and receiving coils, respectively. The air gap between two coils is set as 60 mm [see Fig. 3(c)]. In the prototype, the MRC-based WPT system

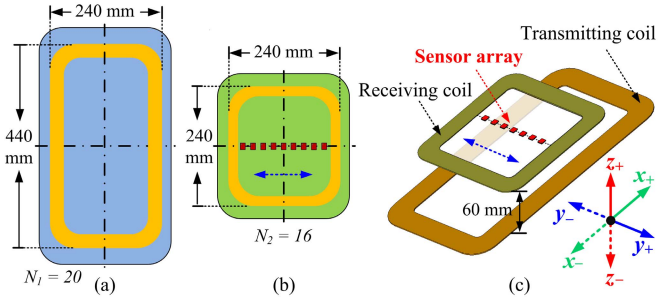

Fig. 3. Geometry of the MRC-based WPT system in both simulation and experiments. (a) Transmitting coil. (b) Receiving coil. (c) 3D view of WPT system with sensor array.

TABLE I
PARAMETERS OF MRC-BASED WPT SYSTEM IN FEM SIMULATION

Parameter	Value
Transmitting coil inductance	252.62 μH
Transmitting coil internal resistance	0.368 Ω
Transmitting coil number of turns	20
Transmitting coil compensation capacitor	0.251 μF
Receiving coil inductance	112.35 μH
Receiving coil internal resistance	0.214 Ω
Receiving coil number of turns	16
Receiving coil compensation capacitor	0.565 μF
Current through transmitting coil	5 A
Operating frequency	20 kHz

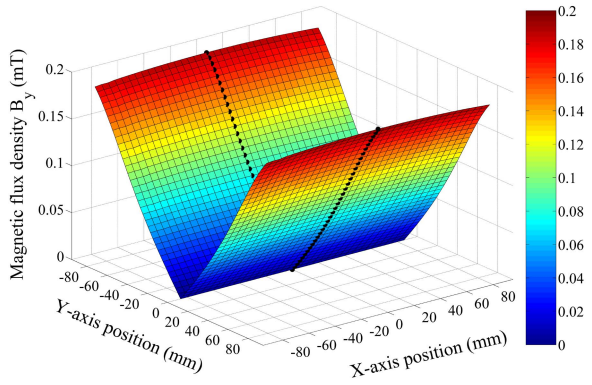

Fig. 4. Simulated y-axis component (B_y) of magnetic field density on the plane of receiving coil when there exists no coil misalignment.

adopts the series–series topology with the operating frequency of 20 kHz. The corresponding key parameters are listed in Table I.

FEM modeling under five different lateral coil misalignment conditions was carried out using JMAG. Fig. 4 shows the simulated y-axis component of magnetic field density (rms value) on the plane of the receiving coil when there exists no coil misalignment (i.e., $\Delta d = 0$ mm). The B_y distribution is symmetric along the y-axis direction. The magnitude of B_y reaches around 0.2 mT at $x = 0$ mm. It is apparent that B_y at the middle position is nearly zero. This simulation result agrees well with (5).

By regulating the lateral coil misalignment (Δd), B_y at the x-axis center line of the receiving coil experiences a

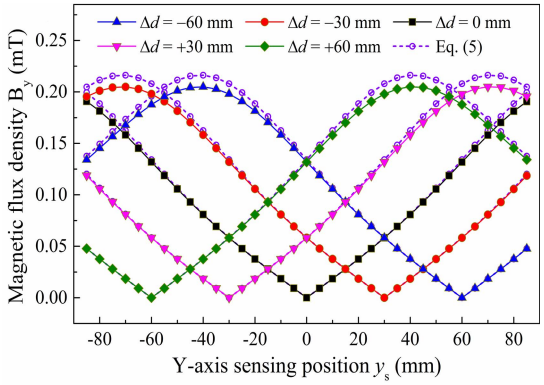

Fig. 5. Simulated y-axis components (B_y) versus sensing positions along the y-axis direction at $x = 0$ mm under five misalignment conditions.

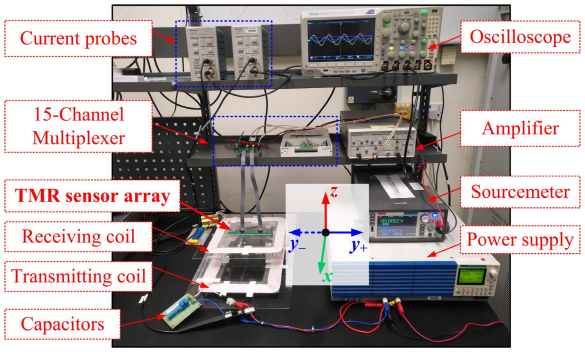

Fig. 6. Experimental prototype of the coil-misalignment detection.

lateral shift, as shown in Fig. 5. When the receiving coil is well aligned with the transmitting coil, the minimum value of the flux density occurs at the y-axis middle position (i.e., $y = 0$ mm). When the receiving coil is misaligned 30 and 60 mm toward the y-direction, the minimum values occur at the y-axis sensing positions of 30 and 60 mm, respectively; on the other hand, when the receiving coil is misaligned 30 and 60 mm toward the y_+ direction, the minimum values occur at the sensing positions of −30 and −60 mm, respectively.

IV. EXPERIMENT AND DISCUSSION

A. Experimental Platform and Sensing Devices

As shown in Fig. 6, the experimental prototype was established according to the simulation parameters as listed in Table I and the geometry as illustrated in Fig. 3. Both the transmitting and receiving coils were made of litz wire. The power source was provided by a bipolar ac power supply (KIKUSUI PBZ40-10). The currents in the transmitting and receiving coils were measured using two wideband current probes (Tektronix TCPA300).

A sensor array consisting of 15 uniaxial TMR sensors uniformly distributed in an interval of 10 mm was mounted on the plane of the receiving coil, as shown in Fig. 7(a). TMR2001 sensor (multidimension) is employed in this paper due to its high sensitivity (i.e., 80 mV/V/mT), compact size (3 mm × 3 mm × 1.45 mm), and wide dynamic range (i.e., up to

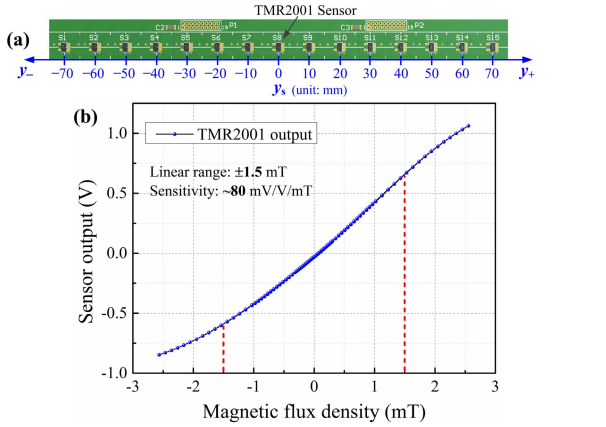

Fig. 7. (a) Design of the sensor array consisting of 15 TMR sensors. The TMR sensors are labeled S1 to S15 along the y-axis direction. (b) Typical characteristic output-field transfer curve of TMR2001 sensor at 2V voltage supply.

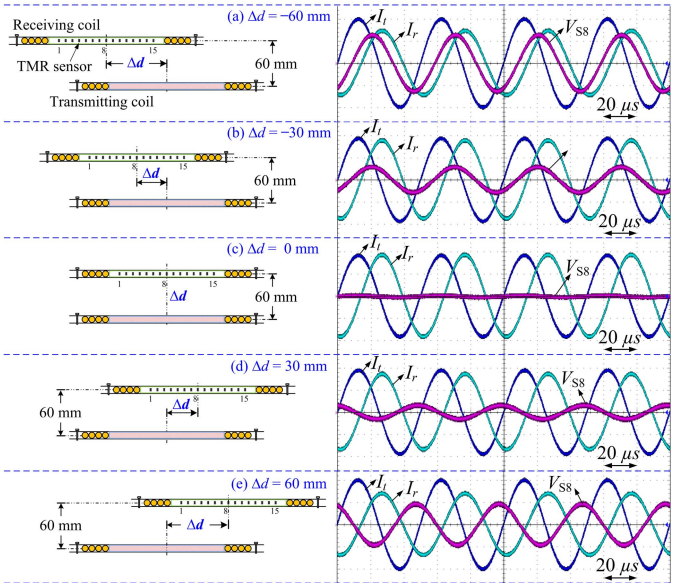

Fig. 8. Measured waveforms of currents in transmitting and receiving coils and sensor signal (S8) under five misalignment conditions [Ch1: I_t (2 A/div), Ch2: I_r (1 A/div), and Ch3: V_{S8} (1 V/div)] (timebase: 20 μs/div).

1 MHz) [16]. This sensor can operate in a linear magnetic field range of ±1.5 mT with a typical output-field transfer curve, as shown in Fig. 7(b). The TMR sensor array was powered by a constant voltage source (Keithley 2400). The outputs from the TMR sensor array were multiplexed by a 15-channel differential multiplexer and then amplified 50 times by a differential voltage preamplifier (SRS SR560). The amplified output signal was captured by an oscilloscope with a sampling rate of 5 MS/s and finally stored in the computer.

B. Experimental Results

By regulating the later misalignment (Δd) of the receiving coil as shown in Fig. 8, the corresponding currents in the transmitting and receiving coils and the output signal from one TMR sensor (S8) at the center position of sensor

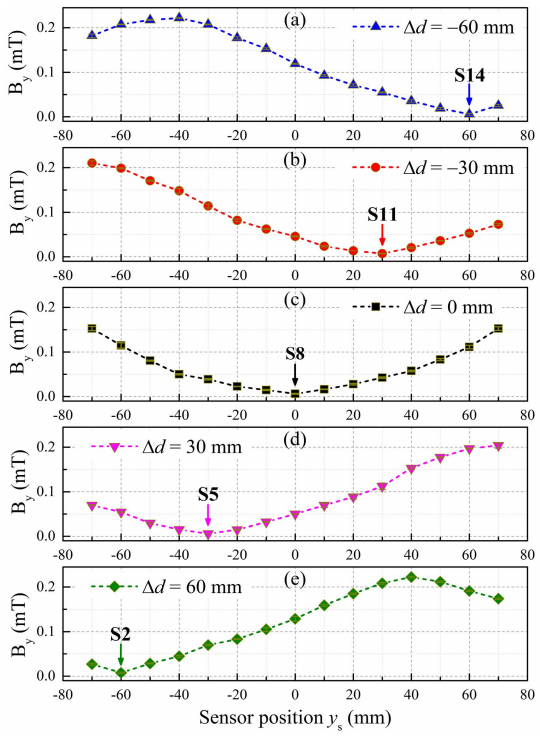

Fig. 9. Measured y-axis component (B_y) of magnetic flux density by the TMR sensor array under five different misalignment conditions. (a) $\Delta d = -60$ mm. (b) $\Delta d = -30$ mm. (c) $\Delta d = 0$ mm. (d) $\Delta d = 30$ mm. (e) $\Delta d = 60$ mm.

array were measured. It can be observed that the magnitude of the current (I_t) through the transmitting coil remained almost constant under five different misalignment conditions, whereas the magnitude of the current through the receiving coil (I_r) gradually decreased as the coil misalignment distance increased. In addition, the output (V_{S8}) of the sensor S8 experiences changes corresponding to the coil misalignment and it becomes almost zero when $\Delta d = 0$ mm, which can match well with (5).

The y-axis component (B_y) of magnetic flux density under five coil misalignment conditions was measured by the sensor array (Fig. 9). The flux density distribution experienced a lateral shift when there existed a coil misalignment. The misalignment position could be determined by the minimal value of the sensor output of the TMR sensor array. In Fig. 9, the measured flux density reached around 0.22 mT. When the receiving coil was well misaligned with the transmitting coil [Fig. 9(c)], the minimum value of approximately 6.2 μT was measured by the sensor S8 (at $y_s = 0$ mm). When the receiving coil was misaligned 30 and 60 mm toward the y_- direction, the minimum output values (i.e., ~7.0 and ~5.7 μT) were measured by the sensor S11 and sensor S14, respectively. Similarly, when the receiving coil is misaligned 30 and 60 mm toward the y_+ direction, the minimum output values (i.e., ~5.8 and ~7.6 μT) of sensor array occur at the position of sensor S5 and sensor S2, respectively. Thus, the coil misalignment (Δd) exhibited a linear relationship with the location on the TMR sensor array where the sensor output is minimal (i.e., nearly zero), as shown in Fig. 10. The sensor

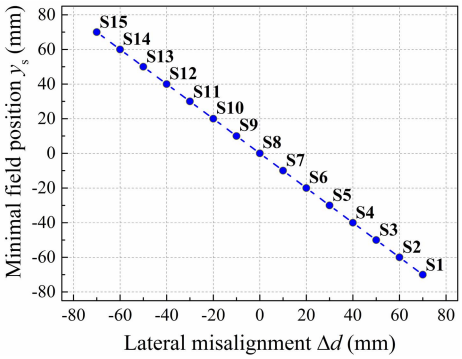

Fig. 10. Linear relationship between the sensor positions corresponding to minimal sensor output and lateral coil misalignment.

array in this paper can provide high-resolution (i.e., 5 mm) measurement results. Therefore, the experimental results agree with the aforementioned theoretical analysis and the FEM simulation results, which further validate the feasibility of the proposed coil-misalignment detection approach. A sensor array with more sensors and smaller interval can provide even more accurate coil misalignment measurement results. Moreover, the exact coil misalignment can be determined by the curve fitting of measured field results in the future work.

V. Conclusion

In this paper, the operating principle of the lateral coil-misalignment detection is introduced and analyzed. A TMR sensor array is utilized to detect the lateral misalignment between the receiving coils and transmitting coil that is highly dependent on the vehicle movement. The 3-D FEM modeling and experimental results using a prototype are presented to validate the effectiveness and feasibility of the proposed approach. This paper provides the theoretical and experimental basis to implement the coil-misalignment detection approach for the DWC system.

Acknowledgment

This work was supported in part by the Seed Funding Program for Basic Research, Seed Funding Program for Applied Research, and Small Project Funding Program from the University of Hong Kong, ITF Tier 3 funding under Grant ITS/203/14, Grant ITS/104/13, and Grant ITS/214/14, in part by RGC-GRF under Grant HKU 17210014 and Grant HKU 17204617, and in part by the University Grants Committee of Hong Kong under Contract AoE/P-04/08.

References

[1] S. Y. Choi, B. W. Gu, S. Y. Jeong, and C. T. Rim, "Advances in wireless power transfer systems for roadway-powered electric vehicles," *IEEE Trans. Emerg. Sel. Topics Circuits Syst.*, vol. 3, no. 1, pp. 18–36, Mar. 2015.

[2] S. Li and C. C. Mi, "Wireless power transfer for electric vehicle applications," *IEEE J. Emerg. Sel. Topics Power Electron.*, vol. 3, no. 1, pp. 4–17, Mar. 2015.

[3] F. Lu, H. Zhang, H. Hofmann, and C. C. Mi, "A dynamic charging system with reduced output power pulsation for electric vehicles," *IEEE Trans. Ind. Electron.*, vol. 63, no. 10, pp. 6580–6590, Oct. 2016.

[4] J. Deng, "Architecture design of the vehicle tracking system based on RFID," *Indonesian J. Elect. Eng. Comput. Sci.*, vol. 11, no. 6, pp. 2997–3004, 2013.

[5] J. I. Hernandez and C. Y. Kuo, "Lateral control of higher order nonlinear vehicle model in emergency maneuvers using absolute positioning GPS and magnetic markers," *IEEE Trans. Veh. Technol.*, vol. 53, no. 2, pp. 372–384, Mar. 2004.

[6] Y.-S. Byun, R.-G. Jeong, and S.-W. Kang, "Vehicle position estimation based on magnetic markers: Enhanced accuracy by compensation of time delays," *Sensors*, vol. 15, no. 11, pp. 28807–28825, 2015.

[7] K. Hwang *et al.*, "An autonomous coil alignment system for the dynamic wireless charging of electric vehicles to minimize lateral misalignment," *Energies*, vol. 10, no. 3, p. 315, Mar. 2017.

[8] K. Hwang *et al.*, "Autonomous coil alignment system using fuzzy steering control for electric vehicles with dynamic wireless charging," *Math. Problems Eng.*, vol. 2015, Nov. 2015, Art. no. 205285.

[9] L. Jogschies *et al.*, "Recent developments of magnetoresistive sensors for industrial applications," *Sensors*, vol. 15, no. 11, pp. 28665–28689, 2015.

[10] P. P. Freitas, R. Ferreira, S. Cardoso, and F. Cardoso, "Magnetoresistive sensors," *J. Phys., Condens. Matter*, vol. 19, no. 16, p. 165221, 2007.

[11] G. A. Covic and J. T. Boys, "Inductive power transfer," *Proc. IEEE*, vol. 101, no. 6, pp. 1276–1289, Jun. 2013.

[12] S. Kim, H.-H. Park, J. Kim, J. Kim, and S. Ahn, "Design and analysis of a resonant reactive shield for a wireless power electric vehicle," *IEEE Trans. Microw. Theory Techn.*, vol. 62, no. 4, pp. 1057–1066, Apr. 2014.

[13] S. Y. Choi, J. Huh, W. Y. Lee, and C. T. Rim, "Asymmetric coil sets for wireless stationary EV chargers with large lateral tolerance by dominant field analysis," *IEEE Trans. Power Electron.*, vol. 29, no. 12, pp. 6406–6420, Dec. 2014.

[14] J. P. W. Chow, N. Chen, H. S. H. Chung, and L. L. H. Chan, "An investigation into the use of orthogonal winding in loosely coupled link for improving power transfer efficiency under coil misalignment," *IEEE Trans. Power Electron.*, vol. 30, no. 10, pp. 5632–5649, Oct. 2015.

[15] J. Kim *et al.*, "Coil design and shielding methods for a magnetic resonant wireless power transfer system," *Proc. IEEE*, vol. 101, no. 6, pp. 1332–1342, Jun. 2013.

[16] *TMR2001 TMR Linear Sensor Datasheet*. Accessed: Mar. 2018. [Online]. Available: http://www.dowaytech.com/en/1944.html